Journal of Metals, Materials and Minerals, 36(1), e2394, 2026

Synergy of ground granulated blast-furnace slag and limestone powder in ternary cement: Effects on heat of hydration and strength development

Pailyn THONGSANITGARN[1,*], Watcharapong WONGKEO[2], Thanongsak NOCHAIYA[3], and Arnon CHAIPANICH[4]

[1] *Applied Physics Program, Faculty of Sciences and Liberal Arts, Rajamangala University of Technology Isan, Nakhon Ratchasima 30000, Thailand*

[2] *Physics and General Science Program, Faculty of Science and Technology, Nakhon Ratchasima Rajabhat University, Nakhon Ratchasima 30000, Thailand*

[3] *Department of Physics, Faculty of Science, Naresuan University, Phitsanulok 65000, Thailand*

[4] *Advanced Cement-Based Materials Research Laboratory, Department of Physics and Materials Science, Faculty of Science, Chiang Mai University, Chiang Mai 50200, Thailand*

***Corresponding author e-mail**: pailyn.th@rmuti.ac.th

Received date:
2 May 2025
Revised date:
8 October 2025
Accepted date:
14 November 2025

Keywords:
Ground granulated blast-furnace slag;
Limestone powder;
Heat of hydration;
Strength;
Cement

Abstract

This study explores the synergistic effect of ground granulated blast-furnace slag (GGBS) and limestone powder (LS) on the hydration behavior and mechanical performance of ternary cement systems. Calorimetry revealed that 30GGBS mix showed a significantly lower peak of about 2.3 $mW \cdot g^{-1}$ and a delayed response. In contrast, the incorporation of LS enhanced early hydration, with the 30LS mix reaching a peak of approximately 2.8 $mW \cdot g^{-1}$ around 6 h. Among ternary blends, 15GGBS–15LS exhibited the highest and earliest heat flow peak (about 2.55 $mW \cdot g^{-1}$ around 7.5 h), while 25GGBS–5LS showed a slower response (about 2.45 $mW \cdot g^{-1}$ around 9.5 h). Despite differences in kinetics, all ternary mixes showed similar cumulative heat at 48 h (226.6 $J \cdot g^{-1}$ to 229.4 $J \cdot g^{-1}$), indicating that GGBS–LS synergy balances early kinetics and total heat evolution. Thermogravimetric analysis confirmed the formation of key hydration phases, including C–S–H, ettringite, monocarboaluminate, and calcium carbonate. The lowest $Ca(OH)_2$ content was found in the 25GGBS–5LS mix, indicating active pozzolanic reaction. The formation of monocarboaluminate phases in ternary systems further indicated chemical synergy between LS and GGBS. At 28 day, the 25GGBS–5LS mix achieved the highest compressive strength of 51.68 MPa, surpassing the control (50.12 MPa), and maintained superior performance up to 180 day. Flexural strength followed a similar trend, the 25GGBS–5LS mixes reaching the highest flexural strength among all ternary blends. A strong linear correlation was found between compressive and flexural strength ($R^2 = 0.906$). These results demonstrate that the synergistic combination of GGBS and LS not only enhances hydration kinetics but also contributes to superior strength development and improved sustainability in blended cement systems. The 25GGBS–5LS formulation was identified as optimal in balancing early hydration and long-term mechanical performance.

1. Introduction

The increasing demand for sustainable construction materials has driven significant interest in alternative binders and supplementary cementitious materials (SCMs) to reduce the environmental impact associated with ordinary Portland cement (PC) production [1–4]. A wide range of industrial by-products and agricultural wastes have been studied as SCMs for their pozzolanic or latent hydraulic properties, contributing to the reduction of cement consumption and promotion of circular economy principles. For example, coal-fired bottom ash has been chemically treated to improve its performance in fiber-reinforced cement composites [5], while bagasse ash and pottery stone have been successfully used in autoclaved lightweight concrete [6]. Porous geopolymers have also been fabricated using aluminum waste as a foaming agent [7], and fly ash from the ASEAN region has been extensively investigated in terms of fineness and calcium oxide content for improving cement–fly ash system properties [8]. Furthermore, recent work has explored power plant waste management (including fly ash, bottom ash, and biomass ash) as part of sustainable construction strategies in emerging economies [9].

Among these alternatives, ground granulated blast-furnace slag (GGBS) and limestone powder (LS) have emerged as promising candidates due to their environmental, economic, and technical benefits [10–13]. GGBS, a by-product of the iron-making industry, possesses latent hydraulic properties that can be activated in the presence of an alkaline environment, such as that provided by PC hydration. The use of GGBS in cement and concrete has been extensively studied, showing improvements in long-term strength development, durability, and resistance to chemical attacks [10]. Furthermore, its utilization supports the principles of a circular economy by transforming industrial waste into valuable construction materials [13].

Limestone powder, on the other hand, has been increasingly recognized not only as an inert filler but also as a material that can participate in physical and chemical interactions within the cementitious matrix [14–16]. Its fine particle size can enhance the packing density, leading to a reduction in porosity and improvement in early-age mechanical properties. Moreover, limestone can participate in the formation of carboaluminate phases through its reaction with aluminate phases from the cement or from cementitious materials [17], contributing to the refinement of the microstructure.

While numerous studies have examined the individual effects of ground granulated blast-furnace slag [10] and limestone powder [14–16] as partial cement replacements, limited research has explored their combined and synergistic behavior in ternary blended systems. Most previous works have either focused on binary blends (e.g., PC–GGBS or PC–LS) or evaluated ternary systems without in-depth analysis of hydration mechanisms and performance outcomes at both early and later ages.

For example, Ma *et al.* [11] studied binary and ternary blends of limestone powder and silica fume. Prakash *et al.* [12] investigated the combined use of GGBS and silica fume in ultra-high-performance concrete. Furthermore, many studies have reported delayed early-age strength when using GGBS due to its slow hydration kinetics [10], but few have proposed solutions to mitigate this limitation effectively.

The novelty of this study lies in its systematic investigation of the synergistic effects between GGBS and LS in a ternary cement system, focusing on both heat of hydration and mechanical performance across different curing ages. By optimizing the ratio of GGBS and LS, this work not only evaluates performance enhancement but also examines hydration kinetics and nucleation effects, providing a more comprehensive understanding. These results demonstrate a pathway for low-carbon, high-performance cementitious material development that explicitly supports the United Nations Sustainable Development Goals (UN-SDGs). This research aligns with Goal 9 (Industry, Innovation and Infrastructure) through the development of innovative green materials, Goal 12 (Responsible Consumption and Production) by promoting the reuse of industrial by-products and conserving virgin raw materials, and Goal 13 (Climate Action) through significantly reducing CO_2 emissions associated with cement production.

The work by Prasittisopin [9] strongly advocates for integrating power plant waste (fly ash, bottom ash, and biomass ash) into the construction industry to foster a circular economy and achieve sustainability targets. This approach supports the UN-SDGs by encouraging the reuse of industrial by-products, conserving natural resources, and developing innovative, low-carbon materials for a sustainable and smart built environment. Therefore, the findings of that study further confirm the global relevance and necessity of utilizing industrial waste, such as GGBS and LS in the present research, to mitigate the environmental impact of construction.

2. Experimental

2.1 Materials

The morphological characteristics of PC, GGBS and LS were examined using scanning electron microscopy (SEM, JEOL JSM-5910LV) at a magnification of 1000x and 2000x, as shown in Figure 1. SEM image reveals that PC particles are angular, irregular in shape, and vary in size. GGBS particles exhibit irregular and angular morphologies, while LS particles display angular shapes with sizes predominantly below 5 μm. The chemical compositions of the powders, determined via X-ray fluorescence (XRF), are summarized in Table 1. PC is mainly composed of calcium oxide (CaO, 63.62 wt%) and silicon dioxide (SiO_2, 20.64 wt%). Minor oxide components include Al_2O_3 (4.85 wt%) and Fe_2O_3 (3.17 wt%), which are associated with the formation of aluminate and ferrite phases. The primary constituents of GGBS include CaO, SiO_2, Al_2O_3, and magnesium oxide (MgO) components typically found in PC. As presented in Table 1, LS primarily consists of CaO at 50.46 wt%, which confirms its origin as a carbonate-based material. However, unlike PC, LS contains very low amounts of reactive components such as SiO_2 (4.38 wt%) and Al_2O_3 (0.92 wt%), classify LS primarily as an inert filler in cement systems, although it may participate in secondary reactions, such as the formation of indicating that it lacks the pozzolanic or hydraulic activity found in other cementitious materials. These chemical characteristics calcium carboaluminates when combined with aluminate phases. The specific gravities of PC, GGBS, and LS were measured to be 3.15, 2.70, and 2.65, respectively.

Figure 2 showed X-ray diffraction (XRD) patterns of PC, GGBS and LS. The XRD pattern of PC shows sharp and well-defined peaks, indicating a crystalline structure composed primarily of tricalcium silicate (C_3S), dicalcium silicate (C_2S), tricalcium aluminate (C_3A), and tetracalcium aluminoferrite (C_4AF). These mineral phases are responsible for the cement's hydraulic behavior. As shown in Figure 2(b), GGBS exhibits a broad hump between 2θ around 20° to 35°, which is indicative of an amorphous or glassy phase. This amorphous nature is primarily responsible for the latent hydraulic and pozzolanic reactivity of GGBS when used in blended cement systems. The XRD pattern of LS showed calcite peaks corresponding to calcium carbonate ($CaCO_3$) according to JCPDS No.72-1937.

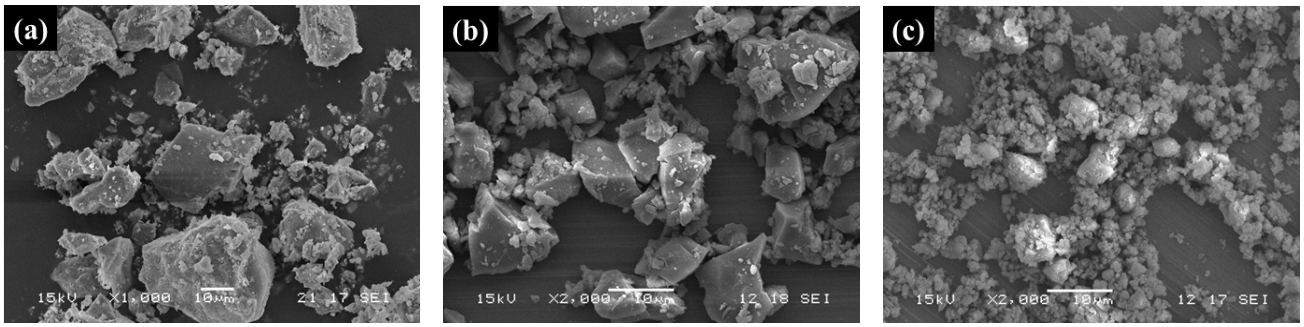

Figure 1. SEM image of particles; (a) PC, (b) GGBS, and (c) LS.

Table 1. Chemical composition of materials used in this study.

Materials	Chemical composition [wt%]								
	SiO_2	Al_2O_3	CaO	Fe_2O_3	MgO	Na_2O	K_2O	SO_3	LOI
PC	20.64	4.85	63.62	3.17	1.14	0.51	0.81	2.75	2.08
GGBS	34.28	11.13	40.59	0.39	8.19	0.02	0.14	3.11	1.54
LS	4.38	0.92	50.46	0.47	0.78	0.02	0.03	0.00	42.85

Table 2. Mix proportions of binary and ternary mixes.

Mix	Proportion [wt%]		
	PC	GGBS	LS
PC	100	-	-
10GGBS	90	10	-
20GGBS	80	20	-
30GGBS	70	30	-
25GGBS–5LS	70	25	5
20GGBS–10LS	70	20	10
15GGBS–15LS	70	15	15
30LS	70	-	30

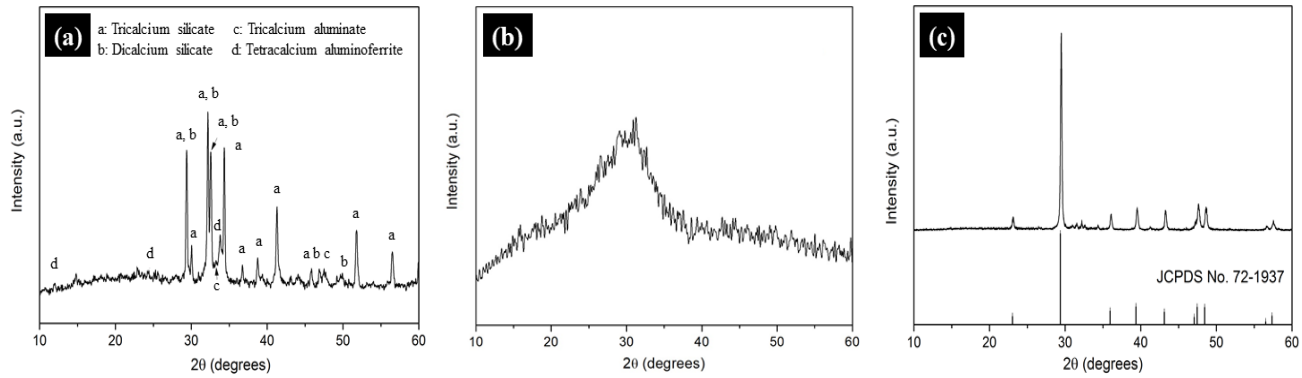

Figure 2. XRD patterns; (a) PC, (b) GGBS, and (c) LS.

Figure 3. Testing equipment: (a) isothermal conduction calorimeter, (b) compressive strength testing machine, and (c) flexural strength testing machine.

2.2 Sample preparation and testing methods

Ground granulated blast-furnace slag and limestone powder were utilized as partial replacements for Portland cement Type I. Portland cement (PC) was replaced by GGBS at 0%, 10%, 20%, and 30% by weight. Further investigations were conducted using a combination of GGBS and limestone powder to replace cement at 30% by weight. The mix proportions are summarized in Table 2.

The heat evolution during the early hydration was monitored using an isothermal conduction calorimeter (I-Cal 4000, Calmetrix, MA, USA), as shown in Figure 3(a). All paste mixtures were prepared at a constant water-to-binder (w/b) ratio of 0.50. Each mix was manually stirred for 30 s before approximately 25 g of the fresh paste was precisely weighed and placed into a calorimeter sample cup. The cups were sealed with plastic lids and immediately inserted into the calorimeter chamber. The heat flow was continuously recorded for the first 48 h of hydration at a controlled temperature of 20°C.

Thermogravimetric analysis (TGA) was conducted on 28 day hydrated pastes using a Mettler Toledo TGA/SDTA 851^e, performed at the National Metal and Materials Technology Center (MTEC),

Thailand. The ground samples were heated from 30°C to 1000°C at a constant heating rate of 20°C·min^{-1} under a nitrogen atmosphere to assess the thermal decomposition and quantify hydration products.

For the mechanical tests, river sand was employed as the fine aggregate. Modified polycarboxylate-based superplasticizer (Sika Viscocrete 10), supplied by Sika (Thailand), was used as a chemical admixture to maintain consistent flow of 110% ± 5% across all mortar mixes for compressive and flexural strength tests.

The compressive strength was evaluated using a compressive strength testing machine (Technotest, MODENA, Italy), as illustrated in Figure 3(b). Mortar cubes with dimensions of 50 mm × 50 mm × 50 mm were tested, and the specimens were prepared following the ASTM C305 standard [18]. A w/b ratio of 0.485 and a fine aggregate-to-binder (a/b) ratio of 2.75 were maintained for all mixes. After casting, the molds were covered with plastic wrap and left in a laboratory environment for 24 h. The specimens were then demolded and cured in lime-saturated water until the designated testing ages. Compressive strength was determined at 1 day, 7 day, 14 day, 28 day, 90 day, and 180 day following ASTM C109 [19], and the results were reported as the average of three specimens.

Flexural strength was evaluated on 28 day mortar prisms in accordance with ASTM C348 [20]. For each mixture, three prisms (40 mm × 40 mm × 160 mm) were prepared using identical mix proportions (w/b = 0.485; a/b = 2.75). The tests were conducted using a universal testing machine (Hounsfield H10KS), as illustrated in Figure 3(c), operated at a crosshead speed of 10 mm·min^{-1}, and the maximum load at failure was recorded to determine the flexural strength.

3. Results and discussion

3.1 Calorimetry

The heat evolution profiles of pastes containing GGBS are presented in Figure 4. The replacement of PC with GGBS significantly reduces the total heat of hydration during the first 48 h and delays the peak heat release compared to plain PC. The control PC exhibits a primary hydration peak of approximately 3.0 mW·g^{-1} occurring at around 10 h. The blends with 10 wt%, 20 wt%, and 30 wt% GGBS showed gradually lower peak values of approximately 2.80 mW·g^{-1}, 2.60 mW·g^{-1}, and 2.30 mW·g^{-1}, respectively. Additionally, the timing of the peak shifted slightly to the right as the GGBS content increased, indicating a slower hydration process. This trend reflects the reduced early-age reactivity of GGBS, which is primarily amorphous and hydrates more slowly than the crystalline phases in Portland cement.

The cumulative heat profiles further confirm this observation. After 48 h, the total heat evolved for the PC mix reached approximately 260 J·g^{-1}, while the 10GGBS and 20GGBS blends achieved around 245 J·g^{-1} and 230 J·g^{-1}, respectively. The 30GGBS paste showed the lowest cumulative heat of 210 J·g^{-1}, reflecting the dilution effect of PC and slower pozzolanic activity of GGBS at early ages.

This behavior is consistent with previous findings [21,22], which attribute the reduced thermal response to the lower reactivity of GGBS. The amorphous, glassy nature of GGBS particles lacks the crystalline phases present in PC, thereby slowing the early hydration process. Additionally, the pozzolanic reaction of GGBS, which involves the secondary formation of calcium silicate hydrate (C–S–H) through the consumption of portlandite ($Ca(OH)_2$), proceeds at a slower rate. These factors contribute to the reduced and delayed thermal output in GGBS-blended systems, particularly during the initial hydration period.

Figure 5 illustrates the heat evolution of cement pastes incorporating GGBS and LS at varying dosages. The heat evolution rate during hydration is presented in Figure 5(a). The incorporation of supplementary cementitious materials significantly alters this profile. Notably, the blend with 30% limestone powder (30LS) shows the most rapid early hydration, reaching a prominent peak heat flow of about 2.8 mW·g^{-1} at an earlier time of approximately 6 h. As shown in Figure 5(b), increasing LS content results in higher cumulative heat release, particularly in the early stages. These findings are consistent with studies by Matschei *et al.* [15] and Thongsanitgarn *et al.* [23], which demonstrated that limestone not only acts as a filler but also contributes chemically to the formation of carboaluminate phases, thereby enhancing the hydration process.

Among the investigated ternary blends, a clear trend related to the GGBS-to-LS ratio is observed. The 15GGBS–15LS mix exhibited the most accelerated hydration, demonstrating the highest and earliest primary heat flow peak at approximately 2.55 mW·g^{-1} occurring around 7.5 h. This accelerated rate directly translated to the cumulative heat release. In contrast, increasing the GGBS content while simultaneously decreasing LS resulted in a delay of hydration. The 20GGBS–10LS blend showed a lower peak heat flow of about 2.5 mW·g^{-1} occurring later, around 8.5 h. The 25GGBS–5LS blend, possessing the highest GGBS and lowest LS content among the ternaries, displayed the lowest and most delayed peak heat flow, reaching only about 2.45 mW·g^{-1} around 9.5 h.

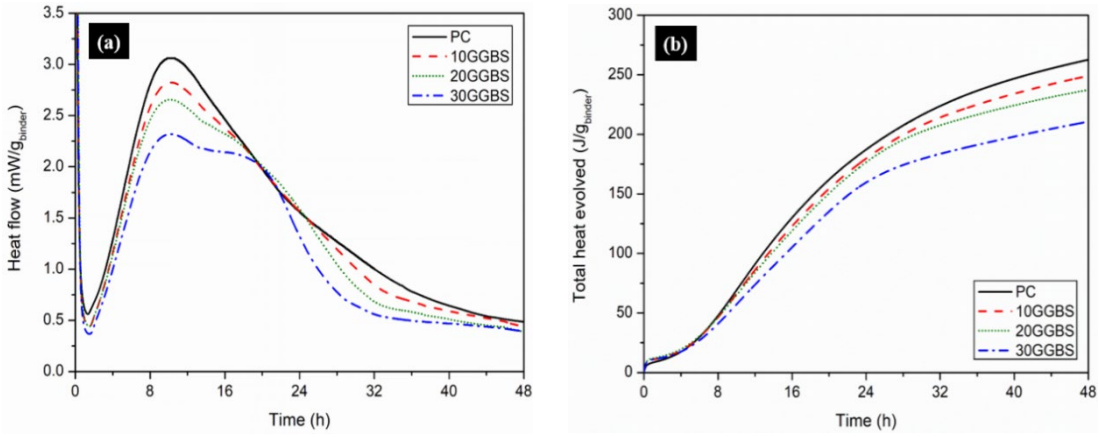

Figure 4. Heat of hydration profiles of PC–GGBS pastes; (a) rate of heat evolution, and (b) cumulative heat release.

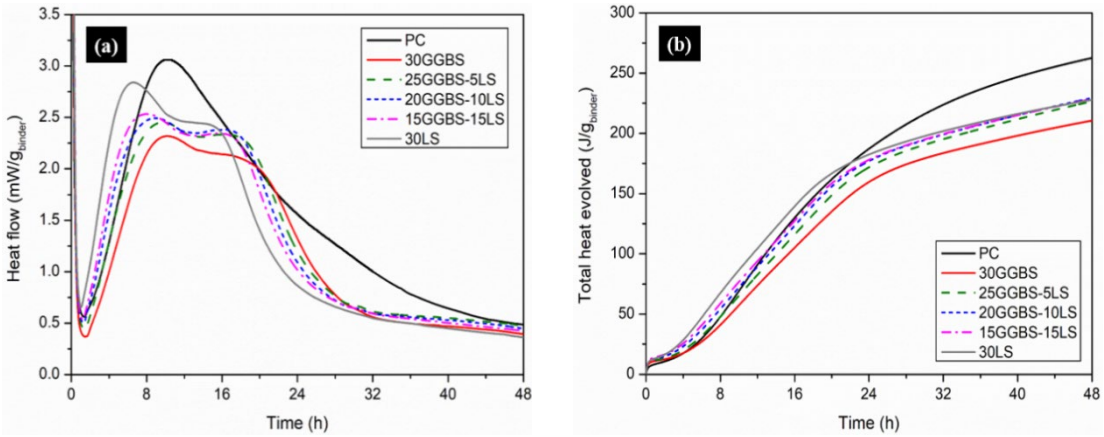

Figure 5. Heat of hydration profiles of PC–GGBS–LS pastes; (a) rate of heat evolution, and (b) cumulative heat release.

However, all ternary blends, namely 25GGBS–5LS (226.6 J·g^{-1}), 20GGBS–10LS (229.4 J·g^{-1}), and 15GGBS–15LS (228.5 J·g^{-1}), exhibit remarkably similar cumulative heat releases by 48 h. This narrow range, spanning from 226.6 J·g^{-1} to 229.4 J·g^{-1}, also closely aligns with the cumulative heat released by the 30LS mix (227.8 J·g^{-1}) at 48 h. This indicates that while the rate of hydration varies among these blends due to the different GGBS-LS ratios, their total extent of hydration over a 48 h period converges to a very consistent range of approximately 225 J·g^{-1} to 230 J·g^{-1}. This suggests that despite differences in early kinetics, the combined pozzolanic and filler effects, coupled with cement dilution, lead to a comparable overall heat generation for these specific formulations.

The synergy between GGBS and LS is evident when both are incorporated together. While GGBS alone delays hydration, the inclusion of LS compensates for this delay by enhancing nucleation and promoting earlier C–S–H formation. This synergistic interaction not only mitigates the dilution effect but also improves early-age hydration kinetics. This observation aligns with the findings of previous studies [24,25], which reported that finely ground limestone acts as a physical filler, providing nucleation sites that promote the formation of hydration products.

3.2 Thermogravimetry

Thermogravimetric analysis was conducted on 28 day cement paste samples incorporating 30% GGBS and LS by mass. The resulting data, presented in Figure 6, quantify phase-specific mass losses. The initial mass loss occurs below 200°C and is attributed to the evaporation of physically adsorbed water and the dehydration of early hydration products such as C–S–H, ettringite (AFt), and monosulfoaluminate (AFm) [26,27]. A second distinct loss between approximately 450°C and 500°C corresponds to the dehydroxylation of calcium hydroxide [$Ca(OH)_2$], or portlandite. A third mass loss, observed between 700°C and 800°C, is associated with the decarbonation of calcium carbonate (calcite).

Figure 7 displays the differential thermogravimetric (DTG) profiles for PC–GGBS–LS ternary blends at 28 day of curing. Five primary mass loss peaks are evident, each representing specific dehydration or decomposition events. Below 100°C, mass loss primarily results from the removal of free and physically adsorbed water within the pore network of the paste [27]. Between 75°C and 95°C, the release of bound water from ettringite leads to the formation of meta-ettringite [28]. Dehydration of C–S–H gel, the dominant hydration product, is reflected in the peak between 100°C and 120°C [29]. As noted by Berodier and Scrivener [14], the presence of fine fillers such as limestone enhances the nucleation of C–S–H, which may increase the prominence of this peak at early ages.

In the range of 150°C to 180°C, the mass loss is associated with the decomposition of carboaluminates formed due to the presence of LS, indicating a reaction between carbonate and aluminate phases. This is supported by findings from De Weerdt *et al.* [25], who identified mono- and hemicarbonate formation around 180°C in LS-containing systems. These results align with the XRD patterns reported by Voglis *et al.* [16], where carboaluminate phases were observed after 24 h of hydration and were shown to increase in abundance through 28 day.

The dehydroxylation of $Ca(OH)_2$ occurs at approximately 450°C to 500°C, releasing water and contributing to a notable mass reduction, consistent with its role as a major hydration product. Finally, a significant mass loss between 700°C and 800°C corresponds to the thermal decomposition of $CaCO_3$ into calcium oxide (CaO) and carbon dioxide (CO_2) [30]. The intensity of this peak increases with higher limestone content, reflecting either unreacted or newly precipitated calcium carbonate.

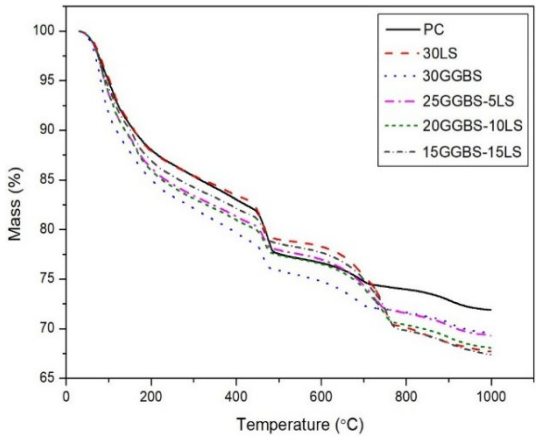

Figure 6. TG curves of PC–GGBS–LS pastes.

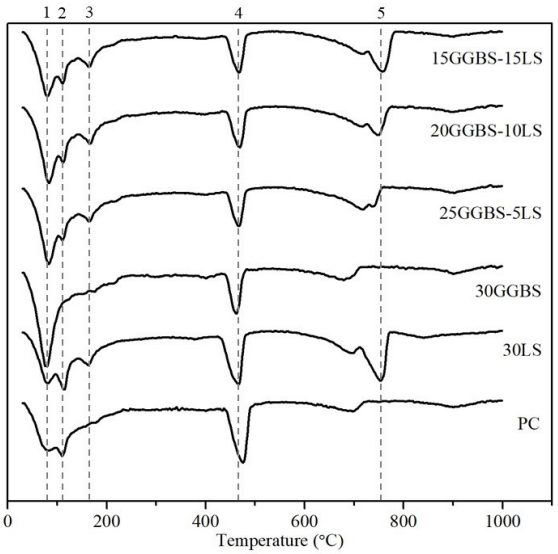

Figure 7. DTG curves of PC–GGBS–LS pastes; 1- free water, 2 - C–S–H, 3 - monocarboaluminate, 4 - $Ca(OH)_2$, 5 - $CaCO_3$.

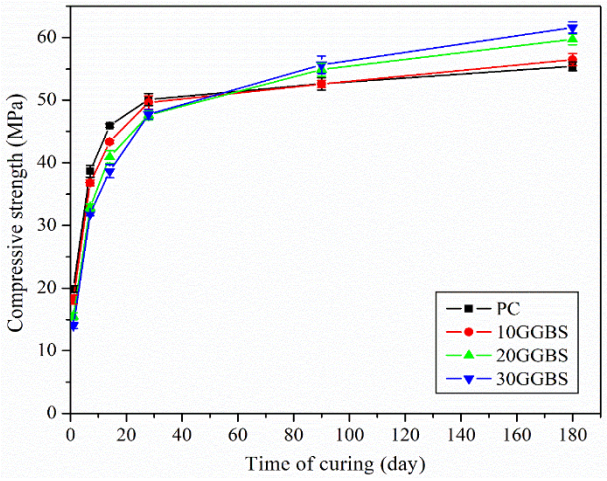

Figure 8. Compressive strength of PC–GGBS mortars.

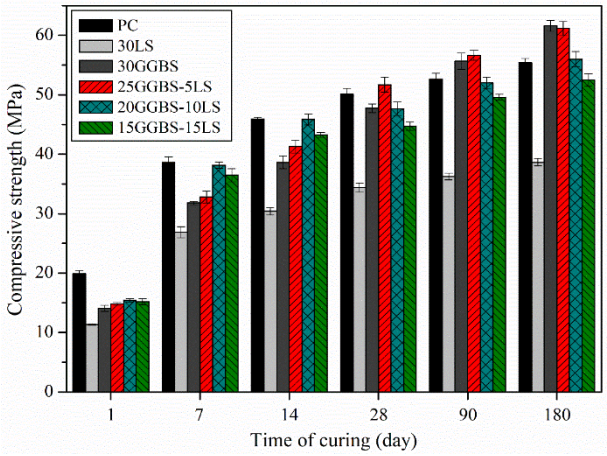

Figure 9. Compressive strength of mortars containing GGBS and LS at 30 wt%.

Thermogravimetric analysis revealed a prominent portlandite peak in the PC paste, which was significantly reduced in blends incorporating GGBS and LS. This reduction can be attributed to both the dilution effect resulting from cement replacement and the pozzolanic activity of GGBS, which consumes portlandite and contributes to the formation of additional C–S–H phases. The presence and intensity of the monocarboaluminate and $CaCO_3$ peaks are more evident in the LS-containing mixes, confirming the formation of carboaluminate phases due to the interaction between LS and aluminate phases.

3.3 Compressive strength

Figure 8 illustrates the development of compressive strength in mortars where PC was partially replaced with GGBS at levels of 10%, 20%, and 30% by weight. At early ages (1 day to 7 day), GGBS-containing mortars exhibited lower compressive strength than the control mix due to the dilution effect and the inherently slower hydration kinetics of GGBS relative to PC. This is consistent with findings by Onn *et al.* [31], who reported that the reduced 28 day compressive strength in GGBS blends was primarily due to the dilution effect and the slower hydration rate of GGBS compared to PC. This resulted in fewer hydration products and, consequently, lower strength than the plain cement mix.

Despite this early-age reduction, the compressive strength of GGBS-blended mortars improved steadily over time, particularly with higher GGBS replacement levels, showing comparable or superior strength to the PC mix at later ages (e.g., 90 day to 180 day). This improvement is attributed to the pozzolanic reaction between the amorphous silica in GGBS and calcium hydroxide ($Ca(OH)_2$), forming additional calcium silicate hydrate (C–S–H), which is the main strength-contributing phase in cementitious systems. These reactions are summarized as follows:

$$\text{Cement} + H_2O \rightarrow \text{C–S–H} + Ca(OH)_2 \quad (1)$$

$$\text{GGBS} + H_2O \rightarrow \text{C–S–H} + Ca(OH)_2 \quad (2)$$

$$Ca(OH)_2 + SiO_2\ (\text{from GGBS}) + H_2O \rightarrow \text{C–S–H} \quad (3)$$

Figure 9 compares the compressive strength of ternary blended mortars containing 30 wt% supplementary cementitious materials (GGBS and LS) with reference binary mixes. The ternary mixes exhibited enhanced compressive strength across all ages tested (1 day to 180 day), particularly the 25GGBS–5LS and 20GGBS–10LS combinations. These mixes not only showed improved early-age strength (1 day and 7 day) compared to binary GGBS systems, but also outperformed PC at later stages (28 day to 180 day).

The observed synergistic effect between GGBS and limestone powder (LS) is likely due to multiple mechanisms. Finely ground LS acts as a physical filler and nucleation site for hydration products, accelerating early hydration and refining the pore structure. Moreover, LS can participate in chemical reactions forming carboaluminate phases, which contribute to microstructural densification and strength development, particularly at later ages. These mechanisms have been confirmed by Antoni *et al.* [32], who studied the combination of metakaolin and limestone as cement substitutes. They found that the reaction between the limestone and the aluminates in metakaolin promotes supplementary AFm phases and stabilizing ettringite, which are beneficial for strength development. This process leads to a denser microstructure and reduced porosity.

Table 3. Flexural strength and compressive strength of mortars after 28 day of curing.

Mix	Flexural strength [MPa]	Compressive strength [MPa]
PC	5.62 ± 0.17	50.12 ± 0.96
10GGBS	5.44 ± 0.10	49.63 ± 1.06
20GGBS	5.56 ± 0.20	47.62 ± 0.76
30GGBS	5.64 ± 0.11	47.73 ± 0.74
25GGBS–5LS	5.58 ± 0.34	51.68 ± 1.26
20GGBS–10LS	5.50 ± 0.36	47.65 ± 1.14
15GGBS–15LS	5.19 ± 0.20	44.73 ± 0.72
30LS	4.77 ± 0.20	34.39 ± 0.76

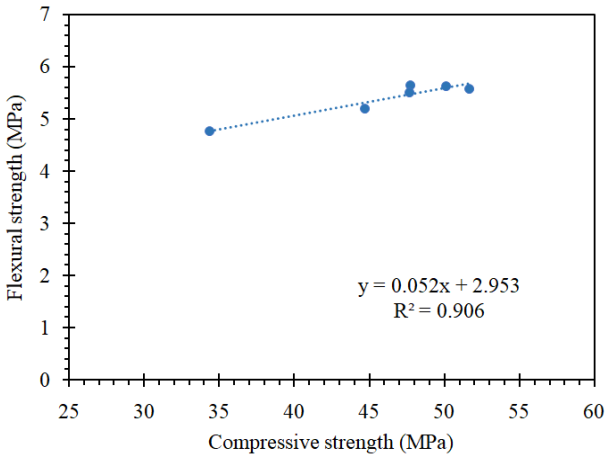

Figure 10. Relationship between flexural strength and compressive strength of mortar mixes with 30% GGBS and LS after 28 day of curing.

Among the ternary systems, the mix containing 25% GGBS and 5% LS yielded the highest strength at both early and later stages, suggesting an optimal balance between pozzolanic reactivity and filler/nucleation effects. In contrast, the 15GGBS–15LS mix showed comparatively lower performance, likely due to excessive dilution of reactive cementitious phases. These results confirm that an appropriate GGBS-to-LS ratio is crucial to maximizing strength performance in ternary blended systems.

3.4 Flexural strength

Table 3 summarizes the flexural and compressive strength results of various mortar mixes after 28 day of curing. The control mix (PC) achieved a compressive strength of 50.12 MPa and a flexural strength of 5.62 MPa, serving as the reference for comparison. Mortars with partial replacement of PC by GGBS showed comparable or slightly reduced strengths depending on the replacement level. Among the binary GGBS mixes, 30GGBS exhibited the highest flexural strength (5.64 MPa), indicating the beneficial effect of GGBS on tensile performance when used at an optimal dosage. Ternary blends incorporating both GGBS and LS demonstrated varying trends. The 25GGBS–5LS mix achieved the highest overall compressive strength (51.68 MPa) and high flexural strength (5.58 MPa), suggesting a synergistic interaction between GGBS and LS. These findings are consistent with the results of other researchers [33-35], such as Menéndez *et al.* [34] and Boubekeur *et al.* [35], who also found that the use of both GGBS and limestone at specific dosages leads to enhanced strength development.

The improvement in flexural strength with certain ternary combinations may be attributed to both the pozzolanic reactivity of GGBS and the filler and nucleation effects of finely ground LS. The synergy between these materials refines the pore structure and promotes a denser and more homogeneous matrix, which contributes to increased tensile load-bearing capacity.

Conversely, mortars containing only LS (30LS) exhibited the lowest flexural strength (4.77 MPa), highlighting the limited contribution of LS when used as a standalone supplementary material. This decline is likely due to the dilution effect and lack of hydraulic reactivity in LS, which primarily serves as a physical filler. The 15GGBS–15LS mix also showed reduced strength, likely caused by excessive cement replacement with non-reactive components, which compromises the formation of load-resisting hydrates.

The relationship between the 28 day compressive and flexural strengths of mortar mixtures with 30% GGBS and LS is presented in Figure 10. A linear regression analysis reveals a strong positive correlation, represented by the equation $y = 0.052x + 2.953$ where y denotes flexural strength and x denotes compressive strength. The coefficient of determination ($R^2 = 0.906$) indicates that approximately 90.6% of the variation in flexural strength can be explained by corresponding changes in compressive strength. This strong relationship suggests that compressive strength can serve as a reliable predictor for flexural strength in blended cement mortars, especially in practical applications where direct flexural testing may not be feasible. The linear trend also highlights the consistent mechanical behaviour of the mortar systems studied, validating the structural integrity of mixes incorporating GGBS and LS.

4. Conclusions

This study investigated the hydration behavior and mechanical performance of ternary blended systems incorporating ground granulated blast-furnace slag (GGBS) and limestone powder (LS). The key conclusions are as follows:

1) The incorporation of GGBS reduced both the peak heat flow and cumulative heat release, with PC showing the highest peak (about 3.0 $mW \cdot g^{-1}$ near 10 h) and 30GGBS the lowest (about 2.3 $mW \cdot g^{-1}$, 210 $J \cdot g^{-1}$ at 48 h). Limestone powder (LS) enhanced early hydration, with 30LS reaching an early peak of approximately 2.8 $mW \cdot g^{-1}$ around 6 h. Among ternary blends, 15GGBS–15LS showed the most accelerated hydration (about 2.55 $mW \cdot g^{-1}$ around 7.5 h), while 25GGBS–5LS had the slowest (about 2.45 $mW \cdot g^{-1}$ around 9.5 h). Despite these differences in hydration rate, all ternary mixes displayed similar cumulative heat release at 48 h (226.6 $J \cdot g^{-1}$ to 229.4 $J \cdot g^{-1}$), indicating that GGBS–LS synergy balances early kinetics and total heat evolution.

2) TGA results revealed that the 25GGBS–5LS mix exhibited the highest C–S–H content, as inferred from the mass loss in the 50°C

to 200°C range, and the lowest $Ca(OH)_2$ residue among all blends. This indicates effective pozzolanic activity and a higher degree of hydration compared to binary systems or the control mix.

3) The compressive strength results showed that mortars with 30% GGBS had improved strength at later ages. Notably, the 25GGBS–5LS mix achieved the highest compressive strength of 51.68 MPa at 28 day, outperforming both the control (50.12 MPa) and other binary or ternary mixes. This highlights the optimal GGBS-to-LS ratio for balancing reactivity and dilution effects.

4) Flexural strength results showed a strong linear correlation with compressive strength ($R^2 = 0.906$). The 30GGBS and 25GGBS–5LS mixes recorded the highest flexural strengths of 5.64 MPa and 5.58 MPa, respectively, indicating improved tensile performance in mixes with optimized ternary combinations.

These findings highlight the importance of optimizing the GGBS-to-LS ratio in ternary systems. A moderate inclusion of LS (10% to 15%) can enhance the early hydration rate, which is beneficial for early-age strength development. On the other hand, a blend with more GGBS and less LS (25GGBS–5LS) may be more advantageous in terms of long-term strength and cumulative hydration.

Acknowledgements

This work (Grant No. RGNS 63-114) was supported by Office of the Permanent Secretary, Ministry of Higher Education, Science, Research and Innovation (OPS MHESI), Thailand Science Research and Innovation (TSRI) and Rajamangala University of Technology Isan. The authors wish to acknowledge the invaluable assistance provided by Ir Prof. Chi Sun Poon and the Concrete Technology Laboratory, Department of Civil and Environmental Engineering, The Hong Kong Polytechnic University in facilitating the use of the calorimeter. The Siam Research and Innovation Co., Ltd. is acknowledged for providing limestone powder and ground granulated blast-furnace slag used in this work.

References

[1] M. Z. Khaiyum, S. Sarker, and G. Kabir, "Evaluation of carbon emission factors in the cement industry: An emerging economy context," *Sustainability*, vol. 15, p. 15407, 2023.

[2] K.-H. Yang, Y.-B. Jung, M.-S. Cho, and S.-H. Tae, "Effect of supplementary cementitious materials on reduction of CO_2 emissions from concrete," *Journal of Cleaner Production*, vol. 103, pp. 774–783, 2015.

[3] B. Lothenbach, K. Scrivener, and R. D. Hooton, "Supplementary cementitious materials," *Cement and Concrete Research*, vol. 41, no. 12, pp. 1244–1256, 2011.

[4] M. E. Shabab, K. Shahzada, B. Gencturk, M. Ashraf, and M. Fahad, "Synergistic effect of fly ash and bentonite as partial replacement of cement in mass concrete," *KSCE Journal of Civil Engineering*, vol. 20, no. 5, pp. 1987–1995, 2016.

[5] P. Sonprasarn, P. Chakartnarodo, P. Ineure, and W. Prakaypan, "Effects of the chemical treatment on coal-fired bottom ash for the utilization in fiber-reinforced cement composites," *Journal of Metals, Materials and Minerals*, vol. 29, no. 4, pp. 55–60, 2019.

[6] S. Sriprasertsuk and S. Daosukho, "Production of autoclaved lightweight concretes using pottery stone and bagasse ash," *Journal of Metals, Materials and Minerals*, vol. 33, no. 2, pp. 53–57, 2023.

[7] S. Chokkha, J. Ayawanna, A. Poowancum, T. Singlaem, and P. Mitsomwang, "Fabrication of porous geopolymers utilizing aluminum wastes as foaming agent," *Journal of Metals, Materials and Minerals*, vol. 34, no. 2, p. 1966, 2024.

[8] T. T. Win, R. Wattanapornprom, L. Prasittisopin, W. Pansuk, and P. Pheinsusom, "Investigation of fineness and calcium-oxide content in fly ash from ASEAN region on properties and durability of cement–fly ash system," *Engineering Journal*, vol. 26, no. 5, pp. 77–90, 2022.

[9] L. Prasittisopin, "Power plant waste (fly ash, bottom ash, biomass ash) management for promoting circular economy in sustainable construction: emerging economy context," *Smart and Sustainable Built Environment*, 2024.

[10] J. Ahmad, K. J. Kontoleon, A. Majdi, M. T. Naqash, A. F. Deifalla, N. Ben Kahla, H. F. Isleem, and S. M. A. Qaidi, "A comprehensive review on the ground granulated blast furnace slag (GGBS) in concrete production," *Sustainability*, vol. 14, p. 8783, 2022.

[11] C. Ma, Z. Yao, Z. Yang, P. Liu, J. Liu, and F. Chen, "Examining the early-stage performance and mechanical performance of limestone powder–silica fume binary cement-based materials," *Case Studies in Construction Materials*, vol. 20, e03010, 2024.

[12] S. Prakash, S. Kumar, R. Biswas, and B. Rai, "Influence of silica fume and ground granulated blast furnace slag on the engineering properties of ultra-high-performance concrete," *Innovative Infrastructure Solutions*, vol. 7, Art. no. 117, 2022.

[13] B. P. Lenka, R. K. Majhi, S. Singh, and A. N. Nayak, "Eco-friendly and cost-effective concrete utilizing high-volume blast furnace slag and demolition waste with lime," *European Journal of Environmental and Civil Engineering*, vol. 26, no. 11, pp. 5351–5373, 2022.

[14] E. Berodier and K. Scrivener, "Understanding the filler effect on the nucleation and growth of C–S–H," *Journal of the American Ceramic Society*, vol. 97, no. 12, pp. 3764–3773, 2014.

[15] T. Matschei, B. Lothenbach, and F. P. Glasser, "The role of calcium carbonate in cement hydration," *Cement and Concrete Research*, vol. 37, no. 4, pp. 551–558, 2007.

[16] N. Voglis, G. Kakali, E. Chaniotakis, and S. Tsivilis, "Portland-limestone cements: Their properties and hydration compared to those of other composite cements," *Cement and Concrete Composites*, vol. 27, no. 2, pp. 191–196, 2005.

[17] K. De Weerdt, M. Ben Haha, G. Le Saout, K. O. Kjellsen, H. Justnes, and B. Lothenbach, "Hydration mechanisms of ternary Portland cements containing limestone powder and fly ash," *Cement and Concrete Research*, vol. 41, no. 3, pp. 279–291, 2011.

[18] ASTM C305-11, "standard practice for mechanical mixing of hydraulic cement pastes and mortars of plastic consistency," *In: Annual Book of ASTM Standard, ASTM International, West Conshohocken, PA,* 2011.

[19] ASTM C109/C109M-20, "Standard test method for compressive strength of hydraulic cement mortars (using 2-in. or [50-mm]

cube specimens)," *In: Annual Book of ASTM Standard, ASTM International*, *West Conshohocken, PA,* 2020.

[20] ASTM C348-08, "Standard test method for flexural strength of hydraulic-cement mortars," *In: Annual Book of ASTM Standard, ASTM International*, *West Conshohocken, PA,* 2008.

[21] H. M. Woo, C. Y. Kim, and J. H. Yeon, "Heat of hydration and mechanical properties of mass concrete with high-volume GGBFS replacements," *Journal of Thermal Analysis and Calorimetry*, vol. 132, pp. 599–609, 2018.

[22] A. M. Neville, *Properties of Concrete*, 4th ed., UK: Addison Wesley Longman, 1997.

[23] P. Thongsanitgarn, W. Wongkeo, A. Chaipanich, and C. S. Poon, "Heat of hydration of Portland high-calcium fly ash cement incorporating limestone powder: Effect of limestone particle size," *Construction and Building Materials*, vol. 66, pp. 410–417, 2014.

[24] P. Thongsanitgarn, W. Wongkeo, and A. Chaipanich, "Hydration and compressive strength of blended cement containing fly ash and limestone as cement replacement," *Journal of Materials in Civil Engineering*, vol. 26, no. 12, p. 04014088, 2014.

[25] K. De Weerdt, K. O. Kjellsen, E. Sellevold, and H. Justnes, "Synergy between fly ash and limestone powder in ternary cements," *Cement and Concrete Composites*, vol. 33, no. 1, pp. 30–38, 2011.

[26] E. T. Stepkowska, J. M. Blanes, F. Franco, C. Real, and J. L. Pérez-Rodríguez, "Phase transformation on heating of an aged cement paste," *Thermochimica Acta*, vol. 420, no. 1–2, pp. 79–87, 2004.

[27] L. Alarcon-Ruiz, G. Platret, E. Massieu, and A. Ehrlacher, "The use of thermal analysis in assessing the effect of temperature on a cement paste," *Cement and Concrete Research*, vol. 35, no. 3, pp. 609–613, 2005.

[28] Q. Zhou, E. E. Lachowski, and F. P. Glasser, "Metaettringite, a decomposition product of ettringite," *Cement and Concrete Research*, vol. 34, no. 4, pp. 703–710, 2004.

[29] A. Bakolas, E. Aggelakopoulou, and A. Moropoulou, "Evaluation of pozzolanic activity and physico-mechanical characteristics in ceramic powder-lime pastes," *Journal of Thermal Analysis and Calorimetry*, vol. 92, pp. 345–351, 2008.

[30] K. Vessalas, P. S. Thomas, A. S. Ray, J.-P. Guerbois, P. Joyce, and J. Haggman, "Pozzolanic reactivity of the supplementary cementitious material pitchstone fines by thermogravimetric analysis," *Journal of Thermal Analysis and Calorimetry*, vol. 97, pp. 71–76, 2009.

[31] C. C. Onn, K. H. Mo, M. K. H. Radwan, W. H. Liew, C. G. Ng, and S. Yusoff, "Strength, carbon footprint and cost considerations of mortar blends with high volume ground granulated blast furnace slag," *Sustainability*, vol. 11, no. 24, p. 7194, 2019.

[32] M. Antoni, J. Rossen, F. Martirena, and K. Scrivener, "Cement substitution by a combination of metakaolin and limestone," *Cement and Concrete Research*, vol. 42, no. 12, pp. 1579–1589, 2012.

[33] M. F. Carrasco, G. Menéndez, V. Bonavetti, and E. F. Irassar, "Strength optimization of 'tailor-made cement' with limestone filler and blast furnace slag," *Cement and Concrete Research*, vol. 35, no. 7, pp. 1324–1331, 2005.

[34] G. Menéndez, V. Bonavetti, and E. F. Irassar, "Strength development of ternary blended cement with limestone filler and blast-furnace slag," *Cement and Concrete Composites*, vol. 25, no. 1, pp. 61–67, 2003.

[35] T. Boubekeur, B. Boulekbache, K. Aoudjane, K. Ezziane, and E.-H. Kadri, "Prediction of the durability performance of ternary cement containing limestone powder and ground granulated blast furnace slag," *Construction and Building Materials*, vol. 209, pp. 215–221, 2019.